Current Commentary

Perovskites and their potential use in solar energy applications

CHRISTOPHER J. RHODES

Fresh-lands Environmental Actions, 88 Star Road, Caversham, Berkshire RG4 5BE, UK
E-mail: cjrhodes@fresh-lands.com

1. Introduction

A material may be described as having a perovskite structure[1] if it has same type of crystal structure as perovskite – calcium titanium oxide ($CaTiO_3$) – does (Figure 1). Perovskite was first discovered in 1839 by Gustav Rose, in the Ural mountains in Russia, and is named after the Russian mineralogist L.A. Perovski (1792–1856), who first characterised the material. The general formula for perovskites is ABX_3, with 'A' and 'B' being two cations of significantly different sizes ('A' > 'B'), while X is an anion that binds with both cations. The perovskite structure is adopted by many oxides that have an elemental composition: ABO_3. The ideal cubic-structure has the 'B' cation in a 6-fold coordination, surrounded by an octahedron of anions, with the 'A' cation in a 12-fold cuboctahedral coordination. Cations 'A' occupy the cube corner positions (0, 0, 0), while cations 'B' occupy the body centred positions (1/2, 1/2, 1/2) with oxygen anions 'O' being located at face centred positions (1/2, 1/2, 0). Figure 1 shows edges for an equivalent unit cell with 'A' in body centre, 'B' at the corners, and 'O' in mid-edge. The requirements of relative ionic radii are quite exacting to maintain a stable cubic structure, meaning that even relatively minor degrees of buckling and distortion can result in
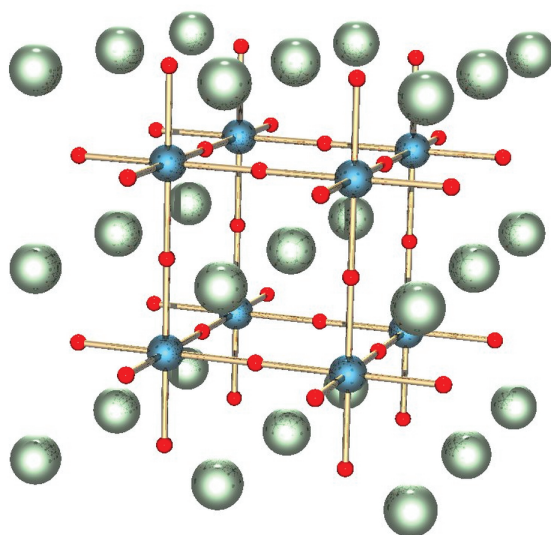

Figure 1 *Structure of a perovskite with a chemical formula ABX_3. The red spheres are X atoms (usually oxygens), the blue spheres are B-atoms (a smaller metal cation, such as Ti^{4+}), and the green spheres are the A-atoms (a larger metal cation, such as Ca^{2+}). Pictured is the undistorted cubic structure; the symmetry is lowered to orthorhombic, tetragonal or trigonal in many perovskites.* http://upload.wikimedia.org/wikipedia/commons/5/54/Perovskite.jpg.

a number of alternative versions with lower symmetry, in which the coordination numbers of either the 'A' cations, 'B' cations, or both, are reduced. Tilting of the BO_6 octahedron reduces the coordination of a too-small 'A' cation from 12 down to as low as 8. Conversely, when a small 'B' cation is brought off-centre, within its octahedral coordination, a stable bonding arrangement can be obtained. Such distortions can create an electric dipole and it is for this reason that perovskites such as $BaTiO_3$, which distort in this manner, exhibit the property of ferroelectricity. The most usual non-cubic forms of perovskites are the orthorhombic and tetragonal variants. There are also some more complex perovskite structures which contain two different 'B'-site cations, with the result that ordered and disordered variants are possible.

Under the high pressure conditions of the Earth's lower mantle, the pyroxene enstatite, $MgSiO_3$, is converted to a more dense perovskite-type polymorph, and indeed it is speculated that this particular phase of the material might be the most common mineral in the Earth[2]. It has a perovskite structure, with an orthorhombic distortion, and is stable at pressures from ~24 GPa to ~110 GPa. [For comparison, the pressure at the centre of the Earth is *ca* 300 GPa.] However, it is stable only at depths of several hundred kilometres and could not be transported back to the Earth's surface without reforming into less dense materials. At yet greater pressures, $MgSiO_3$ perovskite undergoes a transformation to form post-perovskite. Although the most common perovskite compounds contain oxygen, perovskites containing fluoride anions are known, *e.g.* $NaMgF_3$. Metallic perovskite compounds also exist[1], with the general formula RT_3M, where *R* represents a rare-earth or other relatively large cation, *T* is a transition metal ion and *M* represents light metalloids (anions) which occupy the octahedrally coordinated 'B' sites, *e.g.* RPd_3B, RRh_3B and $CeRu_3C$. $MgCNi_3$ is a metallic perovskite compound, and is of particular interest on account of its superconducting properties. A further category has mixed oxide-aurides of Cs and Rb, such as Cs_3AuO, which contain large alkali metal cations in the traditional "anion" sites, bonded to O^{2-} and Au^- anions.

2. Properties of perovskites

As noted, the perovskite structure is imparted with an appreciable element of structural pliancy, and the ideal cubic structure (Figure 1) can be distorted in many different ways. Thus, the octahedra may become tilted, the cations can be displaced from the centres of their coordination polyhedra, and the octahedra might be distorted at the behest of electronic factors (*e.g.* Jahn–Teller distortions)[2]. Accordingly, perovskite materials exhibit many unusual properties that are of theoretical interest, but which may also furnish practical applications. Such phenomena as colossal magnetoresistance, ferroelectricity, superconductivity, charge ordering, spin-dependent transport, high thermopower and the interleaving of structural, magnetic and transport properties are those typically observed from this family of materials. Thus, applications are found for perovskites in sensors and in catalyst electrodes for certain types of fuel cells, and they might play a future role in memory devices and spintronics devices[2]. Many superconducting ceramic materials (high temperature superconductors) have perovskite-like structures, generally incorporating three or more metals, copper often being one of them, and with some prevailing oxygen vacancies. In the latter regard, yttrium barium copper oxide can be made either insulating or superconducting according to its oxygen content. It is also of note that a cobalt-based perovskite material is being developed, intended to replace platinum in the catalytic converters of diesel vehicles[2]. In view of the limited availability of platinum, this would be a major advance. As we shall see, perovskites also offer the potential to be incorporated in efficient, and low-cost photovoltaic cells.

Current Commentary

3. Photovoltaics

The cumulative global photovoltaic generating capacity had reached around $100\,GW_p$ (gigawatts) by the end of 2012, 85% of which was derived from crystalline Si-cells, the remainder being from polycrystalline thin film cells, mostly containing cadmium telluride/cadmium sulfide[3]. While thin-film cells tend to be cheaper to make and offer a shorter energy payback time[4], most of them rely upon rare elements such as tellurium (which is as rare as gold), indium, and gallium, all of which have issues over their future supply[5], certainly if the global photovoltaic generating capacity is to be extended into the Terawatt (TW) realm[3]. On grounds of their relative cheapness and that a conversion efficiency of 15% has been achieved from them (*i.e.* as is competitive with thin-film photovoltaic technology[4]), synthetic perovskites are being explored as foundation materials for the manufacture of high-efficiency commercial photovoltaic devices (*e.g.* Figure 2). As a further convenience, they can be produced using the same thin-film methodology as is used to make thin film silicon solar cells.[6] Organic–inorganic perovskite-structured semiconductors have shown promise as high-performance light-harvesting materials in solar cells, most commonly methylammonium lead triiodide ($CH_3NH_3PbI_3$), initially used as a coating on a mesoporous metal oxide scaffold and more recently as a solid layer in planar heterojunction architectures[6]. Such materials are found to possess both a high charge carrier mobility and a high charge carrier lifetime, meaning that light-generated electrons and holes can move over sufficiently long distances that an electric current may be extracted from them, as opposed to the excitation energy being merely dissipated as heat within the cell. The effective diffusion lengths are close to 100 nm for both electrons and holes in $CH_3NH_3PbI_3$[7,8]. Since low-temperature solution-processed photovoltaics suffer from low efficiencies because of poor exciton or electron-hole diffusion lengths (typically about 10 nanometres), this result is significant and deserves explanation. By applying femtosecond transient optical spectroscopy to bilayers that interface this perovskite with either selective-electron or selective-hole extraction materials, balanced long-range electron-hole diffusion lengths of at least 100 nanometres have been confirmed to exist in solution-processed $CH_3NH_3PbI_3$. It is concluded that the high photoconversion efficiencies of these systems are a result of the fact that the optical absorption length and charge-carrier diffusion lengths are comparable, so obviating the traditional constraints of solution-processed semiconductors[8]. Low-temperature solution methods (spin-coating) are employed for the deposition of the latter
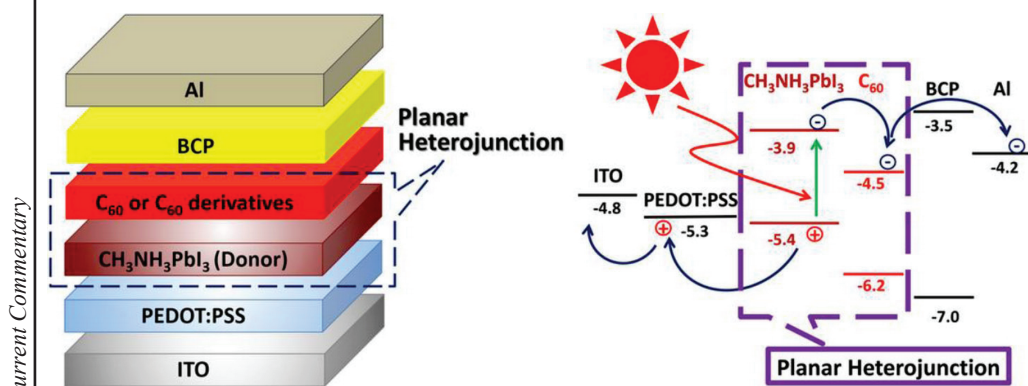

Figure 2 *Diagram showing (left) the device configuration and (right) energy levels of each layer in the device. Al, Aluminium; BCP, bathocuproine; C_{60}, fullerene; PEDOT:PSS, Conducting polymer.*
http://spie.org/Images/Graphics/Newsroom/Imported-2013/005033/005033_10_fig3.jpg

Current Commentary

kind of perovskites. This approach is likely to lead to cheaply produced devices on account of the low temperature solution methods *per se*, and that there is no requirement for rare elements. Solution-processed films produced by other low-temperature (<100 °C) methods have the disadvantage that the resulting diffusion lengths are considerably shorter.

Stranks *et al*.[7] have reported nanostructured photovoltaic cells made with $CH_3NH_3PbI_{3-x}Cl_x$ (essentially the triiodide, but containing a small quantity of chloride) which in one case gave a conversion efficiency of 11.4%, but this was increased to 15.4% when vacuum evaporation was employed. A diffusion length of >1 μm was determined[7] for $CH_3NH_3PbI_{3-x}Cl_x$, which is an order of magnitude greater than that in the pure iodide. The carrier lifetimes were also increased in the mixed halide perovskite from those in the pure iodide[7]. The open-circuit voltage (V_{OC}) typically approaches 1 V in $CH_3NH_3PbI_3$, while for $CH_3NH_3PbI_{3-x}Cl_x$, a $V_{OC} > 1.1$ V has been observed. The band gaps (E_g) of both materials are 1.55 eV, and so the V_{OC}-to-E_g ratios are higher than those usually measured for similar third-generation cells. A V_{OC} of 1.3 V has been demonstrated for perovskites with higher band-gap energies[3]. However, under working conditions, the cell presently lacks sufficient durability to be used as an actual commercial device[3]. New strategies are being explored to obtain an even greater V_{OC}, using $CH_3NH_3PbBr_3$, which, when employed as a film containing Cl^- ions, can be as high as 1.5 V[9]. Vapour-deposition has been employed to make planar heterojunction perovskite solar cells containing simplified device architectures (*i.e.* with complex nanostructures absent), which show a 15% solar-to-electrical power conversion, as determined under simulated full sunlight[6].

The importance of the field is indicated by the recent ACS Selects collection (http://pubs. acs.org/JACSbeta/jvi/issue27.html), and that both the highly reputable journals *Nature* and *Science*, have highlighted[9] perovskite photovoltaics as one of the major scientific advances of the year 2013. On the basis of the rapid developments that have been witnessed in $CH_3NH_3PbX_3$ (X=Cl, Br, or I) perovskite photosensitisers as used in solid-state mesoscopic solar cells, it is anticipated that a power-production efficiency as high as 20% might be obtained, using optimised perovskite-based solid-state solar cells[10]. Indeed, by means of a low-temperature (70 °C) solution processing to make $TiO_2/CH_3NH_3PbI_3$ based solar cells, a power conversion efficiency (PCE) of 13.7% has been obtained, along with a high open circuit potential (V_{OC}) of 1110 mV, which is claimed to be the highest V_{OC} value measured for solution-processed $TiO_2/$ $CH_3NH_3PbI_3$ solar cells. A nanocrystalline TiO_2 (rutile) hole-blocking layer was deposited on a fluorine-doped tin oxide (FTO) conducting glass substrate *via* hydrolysis of $TiCl_4$ at 70 °C, to create an electron-selective contact with the photoactive $CH_3NH_3PbI_3$ film. It was reported that this nanocrystalline rutile is superior in its performance to a planar TiO_2 (anatase) film which was prepared by high-temperature spin coating of $TiCl_4$, and gave a much reduced power conversion efficiency of 3.7%. This result is explained in terms of an intimate junction being formed with a large area, so providing an effective interface between the nanocrystalline rutile TiO_2 and the $CH_3NH_3PbI_3$ layer, with an enhanced ability to extract and mobilise electrons[11]. A series of solution-processed perovskite solar cells based on methylammonium (MA) lead halide derivatives, $MAPbX_3$, has been prepared whose optical properties may be tuned according to the nature and ratio of the halides employed (X=Cl, Br, and I), and with different cell architectures: thin film, and mesoporous scaffold (TiO_2 and Al_2O_3). Using impedance spectroscopy, it is found that the charge recombination rates are decreased in the light absorber film, when Cl and Br are included in the perovskite lattice. The charge recombination rates are lower, as prepared on a mesoporous Al_2O_3 electrode, than those devices prepared on mesoporous TiO_2. In all the devices measured, an efficiency was preserved to at least 80% of the initial value one month after their preparation[12].

282

4. Theoretical and spectroscopic studies of perovskites

The low-frequency resonant Raman spectrum of methylammonium lead-triiodide, adsorbed on mesoporous Al_2O_3 has been obtained. On the basis of DFT calculations of appropriate related systems, the bands at 62 cm^{-1} and 94 cm^{-1} are assigned respectively to the bending and stretching vibrations of the Pb−I bonds, while the bands at 119 cm^{-1} and 154 cm^{-1} are ascribed to librations of the organic cations. There is also a broad, unstructured band spanning the range 200−400 cm^{-1} which is assigned to torsional vibrations of the methylammonium cations, which serves as a marker of the orientational disorder of the material[13]. Electronic structure calculations have been employed to interpret the fundamental properties of bulk perovskites. Hybrid perovskites are predicted to show spontaneous electric polarisation, a phenomenon which might be fine-tuned according to the selection of the organic cation. It is concluded that the presence of ferroelectric domains will form internal junctions that might assist the separation and segregation of photoexcited electron and hole pairs, with an according lowering of the recombination rate. The Wannier−Mott exciton separation and effective ionisation of donor and acceptor defects are both promoted as a result of high dielectric constant and low effective mass, and it is proposed that the photoferroic effect could also be used to generate a higher open circuit voltage in nanostructured films and may be responsible for the current−voltage hysteresis that is measured in perovskite solar cells[14]. Photovoltaic conversion in high-performing perovskite-based mesostructured solar cells has been determined, with a particular focus on the part played by the mesoporous oxide−perovskite interface. Using a number of different spectroscopic methods, in particular Stark spectroscopy, the existence of oriented permanent dipoles, consistent with the hypothesis of an ordered perovskite layer, close to the oxide surface, has been demonstrated. It is concluded that one of the decisive reasons for the highly efficient transport of electrons and holes in perovskite films, could be the presence of such interfacial ordering, as promoted by specific local interactions[15]. The electronic structure and chemical composition that may be deduced using efficient photoelectron spectroscopy with hard X-rays, was used to study $CH_3NH_3PbI_3$ perovskite solar cell materials deposited onto mesoporous TiO_2, so being able to measure the occupied energy levels of the perovskite in addition to those of the underlying TiO_2, so to determine the energy level matching at the interface. A good agreement was found between the simulated density of states and the measured valence levels, and it was concluded that similar electronic structures were formed, despite two different deposition methods being used[16]. DFT calculations have been employed to investigate the intrinsic defects in $CH_3NH_3PbI_3$ and their relation to its photovoltaic properties. Schottky defects, as are vacancies on PbI_2 and CH_3NH_3I, do not form stable trapping sites, and so they can reduce the lifetime of carriers. However, vacancies on Pb, I, and CH_3NH_3 which originate from Frenkel defects, can act as dopants, such that methylammonium lead halides (MALHs) can become unintentionally doped. That there are no intrinsic defects in MALHs is accounted for by the ionic bonding that results from organic−inorganic hybridisation[17].

By means of highly sensitive photothermal deflection and photocurrent spectroscopies, the absorption spectra of $CH_3NH_3PbI_3$ perovskite thin films were measured at room temperature, yielding a high absorption coefficient with an unusually sharp onset. The presence of a well-ordered microstructure is suggested by the fact that below the bandgap, the absorption is exponential over more than four decades and the Urbach energy is down to 15 meV. No evidence for deep states was found at least at the detection limit of ∼1 cm^{-1}. These results accord with the well-established electronic properties of perovskite thin films,

and the relatively high open-circuit voltages measured for perovskite solar cells. Evidence for a change in the composition of the material, caused by the deliberate introduction of moisture, is given by the strong reduction in the absorption at photon energies below 2.4 eV[18]. It has been shown that trap states at the perovskite surface give rise to charge accumulation and consequent recombination losses in working solar cells. It is found that undercoordinated iodine ions within the perovskite structure are responsible for this effect, and supramolecular halogen bond complexation can be utilised as a means to passivate these sites successfully. Thus, solar cells are fabricated with a maximum power conversion efficiency of 15.7% and a stable power output of > 15%, under a constant 0.81 V forward bias, in simulated full sunlight. It is concluded that such means of surface passivation may pave the way to constructing more efficient perovskite solar cells[19]. On the basis of DFT calculations, it is shown that that the band gap in three-dimensional (3D) hybrid perovskites $CH_3NH_3PbX_3$ (X = Br, I) is dominated by a massive spin−orbit coupling (SOC) in the conduction-band (CB). Both direct and isotropic optical transitions, at ambient temperature, are associated with a spin−orbit split-off band that is related to the CB of the cubic lattice which is triply degenerate in the absence of SOC. As a result of the dominance of the SOC, the electronic states involved in the optical absorption are but weakly perturbed by local lattice distortions[20]. Again using DFT calculations, the observed absorption blue shift along the I→Br→Cl series was accounted for in $CH_3NH_3PbX_3$ and mixed halide $CH_3NH_3PbI_2X$ perovskites (X = Cl, Br, I). It was found that $CH_3NH_3PbI_3$ and the mixed $CH_3NH_3PbI_2Cl$ or $CH_3NH_3PbI_{3-x}Cl_x$ perovskites exhibited a similar absorption onset at ~800 nm, whereas $CH_3NH_3PbI_2Br$ absorbs light below ~700 nm. A good accord was met between the calculated band structures and the experimental trend of optical absorption frequencies. The existence of two different structural types with different electronic properties was indicated for the mixed perovskites ($CH_3NH_3PbI_2X$), with a relative stability that depended on the nature of the group, X. For these systems, the calculated energies of formation decrease in the order I > Br > Cl, which would accord with the observed miscibility of $CH_3NH_3PbI_3$ and $CH_3NH_3PbBr_3$, while suggesting that the degree of chlorine incorporation into $CH_3NH_3Pb(I_{1-x}Cl_x)_3$ should be smaller. The calculations further indicate that that in the PbI_4X_2 octahedra, the Cl atoms preferentially occupy the apical positions while Br atoms may occupy both apical and equatorial positions, in agreement with reported lattice parameters[21]. Transient laser spectroscopy and microwave photoconductivity measurements were made[22] on TiO_2 and Al_2O_3 mesoporous films impregnated with $CH_3NH_3PbI_3$ perovskite and the organic hole-transporting material spiro-OMeTAD. The results show that primary charge separation occurs at both junctions, involving simultaneously TiO_2 and spiro-OMeTAD, with ultrafast electron and hole injection occurring from the photoexcited perovskite over similar timescales. It is observed that charge recombination is appreciably slower on TiO_2 films than on Al_2O_3.

5. Technical innovations for transformative perovskite solar cells

A low-temperature vapour-assisted solution process has been introduced[23] to make polycrystalline perovskite thin films with full surface coverage, small surface roughness, and up to microscale grain sizes. Thus, it should be possible to fabricate perovskite films and devices in a simple and highly reproducible fashion. A power conversion efficiency of 12.1% has been achieved, which is the best so far obtained from $CH_3NH_3PbI_3$ using a planar heterojunction configuration, and the critical kinetic and thermodynamic parameters attendant to the film growth were also investigated[23]. A method has been reported for the preparation

of 6 nm-sized nanoparticles of $CH_3NH_3PbBr_3$ perovskites, which employs an ammonium bromide containing a chain of sufficient length (steric size) that the nanoparticles remain dispersed in a wide range of organic solvents. Since the nanoparticles are stable both in the solid state and in concentrated solutions, with no requirement for a mesoporous support, homogeneous nanoparticle thin films can be made by spin-coating onto a quartz substrate. Since both the colloidal solution and the thin film emit light over a narrow wavelength region of the visible spectrum and with a high quantum yield (*ca* 20%), it is thought that the nanoparticles might find particular applications in the fabrication of optoelectronic devices[24]. In $(CH_3NH_3)PbI_3$-sensitised solar cells containing iodide-based electrolytes, $(CH_3NH_3)PbI_3$ is relatively stable in a nonpolar solvent, such as ethyl acetate, so long as the iodide concentration is kept low (*e.g.*, 80 mM). According to frequency-resolved modulated photocurrent/photovoltage spectroscopy when the TiO_2 film thickness is increased from 1.8 to 8.3 μm, the transport is barely altered, but the electron–hole recombination is increased by a factor of >10, which reduces the electron diffusion distance from 16.9 to 5.5 μm. An explanation for this is the greater degree of iodide depletion within the TiO_2 pores as the film thickness increases. Thus, for the development of $(CH_3NH_3)PbI_3$ or similar perovskites in potential photoelectrochemical applications, it will be necessary to find alternative, compatible redox electrolytes[25]. In another study, the effect of TiO_2 film thickness on charge transport and recombination in solid-state mesostructured perovskite $CH_3NH_3PbI_3$ (*via* one-step coating) solar cells, using spiro-MeOTAD as the hole conductor, has been investigated using intensity-modulated photocurrent/photovoltage spectroscopies. It is demonstrated that charge transport in perovskite cells is not dominated by electron conduction from the perovskite layer, but within the mesoporous TiO_2 network. The film-thickness was found to have little influence on the electron-hole transport and recombination processes, and yet the efficiency of perovskite cells increases as the TiO_2 film increases in thickness from 240 nm to *ca* 650–850 nm. This effect is a consequence of enhanced light harvesting by the thicker films, although a drop-off in the cell efficiency is found as the film thickness is further increased, which is thought to be connected with a reduced fill factor or photocurrent density[26]. A novel metal-halide perovskite has been produced, based on the formamidinium cation ($HC(NH_2)_2^+$), which displays a favourable band gap (1.47 eV) and has a broader absorption than light absorbing materials that contain the methylammonium cation ($CH_3NH_3^+$), as previously documented. The high open-circuit voltage ($V_{oc} = 0.97$ V) and promising fill-factor (FF = 68.7%) yield an efficiency of 4.3%. The formation of a black trigonal (*P3m*1) perovskite polymorph and a yellow hexagonal nonperovskite (*P63mc*) polymorph is also reported, and it is concluded that to develop the cell further would necessitate the stabilisation of the black trigonal (*P3m*1) perovskite polymorph over the yellow hexagonal nonperovskite (*P63mc*) polymorph[27].

Perovskite $(CH_3NH_3)PbI_3$-sensitised solid-state solar cells have been reported which contain spiro-OMeTAD, poly(3-hexylthiophene-2,5-diyl) (P3HT) and 4-(diethylamino) benzaldehyde diphenylhydrazone (DEH) as hole transport materials (HTMs), which yield a respective light-to-electricity conversion efficiency of 8.5%, 4.5%, and 1.6%, under AM 1.5 G illumination with an intensity of 1000 W m^{-2}. Measurements made using photoinduced absorption spectroscopy (PIA) show that the hole transfer occurs from the $(CH_3NH_3)PbI_3$ to the particular HTM, following an initial excitation of $(CH_3NH_3)PbI_3$. The electron lifetimes (τ_e) in these devices decrease in the order spiro-OMeTAD > P3HT > DEH, so explaining the lower efficiency of the cells containing P3HT and DEH; however, the charge transport time (t_{tr}) is relatively insensitive to the nature of the HTM[28]. Copper iodide (CuI) has emerged as a potential new inorganic hole conducting material for perovskite-based thin film photovoltaics,

since it has been used in a cell to yield a power conversion efficiency of 6.0%, and with excellent photocurrent stability. However, the open-circuit voltage is much lower than is obtained from the best spiro-OMeTAD devices, as is attributed to a higher degree of recombination in CuI devices, according to results obtained from impedance spectroscopy. However, the latter technique also disclosed that the electrical conductivity in CuI is two orders of magnitude higher than in spiro-OMeTAD, meaning that significantly greater fill factors are possible[29]. The optical and electronic structures of three N,N-di-p-methoxyphenylamine-substituted pyrene derivatives were investigated by UV-Vis spectroscopy and cyclic voltammetry, to be used as hole-transporting materials (HTMs) in mesoporous TiO_2/$CH_3NH_3PbI_3$/HTMs/Au solar cells. A short-circuit current density of 20.2 mA cm^{-2}, an open-circuit voltage (V_{oc}) of 0.886 V, and a fill factor of 69.4% were measured under an illumination of 1 sun (100 mW cm^{-2}), which gave an overall light to electricity conversion efficiency of 12.4%. Accepting that the V_{oc} is slightly lower, the performance of the pyrene analogue is comparable with that of the well-studied spiro-OMeTAD, and may find future applications as an HTM in perovskite-based solar cells[30].

A feature article on perovskite solar cells was published in the September 2014 issue of the Royal Society of Chemistry's flagship magazine, *Chemistry World*[31].

References

1. Wenk, H.-R. and Bulakh, A. (2004) *Minerals: their constitution and origin*. Cambridge University Press, New York.
2. http://en.wikipedia.org/wiki/Perovskite_%28structure%29.
3. Hodes, H. (2013) Perovskite-based solar cells. *Science*, **343**, 317–318.
4. Rhodes, C.J. (2010) Solar energy: principles and possibilities. *Sci. Prog.*, **93**, 37–112.
5. Rhodes, C.J. (2011) Shortage of resources for renewable energy and food production. *Sci. Prog.*, **94**, 323–334.
6. Liu, M. *et al.* (2013) Efficient planar heterojunction perovskite solar cells by vapour deposition. *Nature,* **501 (7467)**, 395–398.
7. Stranks, S.D. *et al.* (2013) Electron-hole diffusion lengths exceeding 1 micrometer in an organometal trihalide perovskite absorber. *Science*, 342, 341–344.
8. Xing, G. *et al.* (2013) Long-range balanced electron- and hole-transport lengths in organic-inorganic $CH_3NH_3PbI_3$. *Science*, 342, 344–347.
9. Kamat, P.V. (2014) Organometal halide perovskites for transformative photovoltaics. *J. Am. Chem. Soc.*, **136**, 3713–3714.
10. Park, N.-G. (2013) Organometal perovskite light absorbers toward a 20% efficiency low-cost solid-state mesoscopic solar cell. *J. Phys. Chem. Lett.*, **4**, 2423–2429.
11. Yella, A. *et al.* (2014) Nanocrystalline rutile electron extraction layer enables low-temperature solution processed perovskite photovoltaics with 13.7% efficiency. *Nano Lett.*, **14**, 2591–2596.
12. Saurez, B. *et al.* (2014) Recombination study of combined halides (Cl, Br, I) perovskite solar cells. *J. Phys. Chem. Lett.*, **5**,1628–1635.
13. Quarti, C. *et al.* (2014) The Raman spectrum of the $CH_3NH_3PbI_3$ hybrid perovskite: Interplay of Theory and Experiment. *J. Phys. Chem. Lett.*, **5**(2), 279–284**.**
14. Frost, J.M. *et al.* (2014) Atomistic origins of high-performance in hybrid halide perovskite solar cells. *Nano Lett.*, **14**, 2584–2590.
15. Roiati, V. *et al.* (2014) Stark effect in perovskite/TiO_2 solar cells: evidence of local interfacial order. *Nano Lett.*, **14**, 2168–2174.
16. Lindblad, R. *et al.* (2014) Electronic structure of TiO_2/$CH_3NH_3PbI_3$ perovskite solar cell interfaces. *J. Phys. Chem. Lett.*, **5**, 648–653.
17. Kim, J. *et al.* (2014) The role of intrinsic defects in methylammonium lead iodide perovskite. *J. Phys. Chem. Lett.,* **5**, 1312–1317.
18. De Wolff, S. *et al.* (2014) Organometallic halide perovskites: sharp optical absorption edge and its relation to photovoltaic performance. *J. Phys. Chem. Lett.*, **5**, 1035–1039.

19. Abate, A. *et al*. (2014) Supramolecular halogen bond passivation of organic–inorganic halide perovskite solar cells. *Nano Lett*., Article ASAP DOI: 10.1021/nl500627x http://pubs.acs.org/doi/abs/10.1021/nl500627x.

20. Even, J. *et al*. (2013) Importance of spin–orbit coupling in hybrid organic/inorganic perovskites for photovoltaic applications. *J. Phys. Chem. Lett.*, **4**, 2999–3005.

21. Mosconi, E. *et al*. (2013) First-principles modeling of mixed halide organometal perovskites for photovoltaic applications. *J. Phys. Chem. C.*, **117**, 13902–13913.

22. Marchioro, A. *et al*. (2014) Unravelling the mechanism of photoinduced charge transfer processes in lead iodide perovskite solar cells. *Nature Photonics*, 8, 250–255.

23. Chen, Q. *et al*. (2014) Planar heterojunction perovskite solar cells *via* vapor-assisted solution process. *J. Am. Chem. Soc.*, **136**, 622–625.

24. Schmidt, L.C. *et al*. (2014) Nontemplate synthesis of $CH_3NH_3PbBr_3$ perovskite nanoparticles. *J. Am. Chem. Soc.*, **136**, 850–853.

25. Zhao, Y. and Zhu, K. (2013) Charge transport and recombination in perovskite $(CH_3NH_3)PbI_3$ sensitized TiO_2 solar cells. *J. Phys. Chem. Lett.*, **4**, 2880–2884.

26. Zhao, Y. *et al*. (2014) Solid-state mesostructured perovskite $CH_3NH_3PbI_3$ solar cells: charge transport, recombination, and diffusion length. *J. Phys. Chem. Lett.*, **5**, 490–494.

27. Koh, T.M. *et al*. (2013) Formamidinium-containing metal-halide: an alternative material for near-IR absorption perovskite solar cells. *J. Phys. Chem. C.*, Article ASAP DOI: 10.1021/jp411112k.

28. Bi, D. *et al*. (2013) Effect of different hole transport materials on recombination in $CH_3NH_3PbI_3$ perovskite-sensitized mesoscopic solar cells. *J. Phys. Chem. Lett.*, **4**, 1532–1536.

29. Christians, J.A. *et al*. (2014) An inorganic hole conductor for organo-lead halide perovskite solar cells. Improved hole conductivity with copper iodide. *J. Am. Chem. Soc.*, **136**, 758–764.

30. Jeon, N.J. *et al*. (2013) Efficient inorganic–organic hybrid perovskite solar cells based on pyrene arylamine derivatives as hole-transporting materials. *J. Am. Chem. Soc.*, **135**, 19087–19090.

31. Extance, A. (2014) The power of perovskites. *Chemistry World*, **11**, 46-49.

Current Commentary